P. N. Slater
R. A. Schowengerdt
University of Arizona
Tucson, Arizona 85721

Sensor Performance for Earth Resource Studies

This approach to the analysis of earth resources imagery may provide some of the important basic data needed by those responsible for planning the missions.

Introduction

Recently Rosenberg[1] mentioned the effort of COSPEAR[2] to "determine reasonable system performance requirements of various types of users in the earth resources survey programs." However, neither he nor others concerned with this problem have proposed a solution. We believe a solution can be developed and have been attempting to refine one particular approach, which we outline here. Although this solution is aimed primarily at the evaluation of photographic and infrared imagery from spacecraft, it could be applied to other forms of imagery and to high-altitude aircraft or balloon platforms.

A problem that has beset the earth resources program from its inception has been how to quantitatively determine the spatial resolution or spatial information content of the data collected. Many discussions have centered on the question of how much spatial resolution is required for a given discrimination or identification to be made. The question itself has a qualified, relative answer. The qualifications concern factors such as the degradation in image quality caused by the atmosphere, and the relative nature of the answer is due to the lack of an absolute relationship between resolution and information content. For these reasons we do not believe that the characterization of imagery in terms of spatial resolution or spatial frequency content will be adequate. We believe a more promising approach is first to use the spatial frequency content of the imagery to determine the inflight modulation transfer function (MTF) of the sensor and then for the earth scientist to use the statistical results of visual or machine-aided photointerpretation to establish the relationship between the sensor MTF and the quantity and quality of earth resources data extractable from the imagery. How the effect of the atmosphere can be accounted for is described at the end of this communication.

Parenthetically, a knowledge of the inflight MTF of the sensor, *excluding* variable atmospheric effects, can also be used to determine how well the sensor is operating compared to preflight laboratory MTF measurements and to determine the extent of any changes in performance during the experiment lifetime. The same procedure can be used to determine the image degradation introduced in the various photographic duplication steps employed.

The inflight MTF of a sensor, including the effects of the atmosphere, can be determined from edge gradient analyses. This has, in fact, been attempted for some early Gemini photography. However, high-quality straight edges are rare in space photography, and often an apparently good edge is accompanied by a narrow boundary region. For example, between *land* and *sea* there is the beach; between large cultivated fields there is a farm road. These narrow regions may not

ABSTRACT: *The spatial frequency content of earth resources imagery is related to the inflight modulation transfer function of the sensor. Through the statistical results of visual or machine-aided photointerpretation, the relationship between the sensor MTF and the quantity and quality of the extractable earth resources data can be established. The results can form the basis for the specification of sensor performance in future earth resources missions.*

be visible in the imagery, but they disrupt the object intended to be used as the edge and result in erroneous values of the MTF obtained by edge gradient analysis.

The correlation and power spectrum analysis approach that we propose to use to determine the MTF has the advantages of independence of object scene, insensitivity to film granularity and scan raster pattern relative to other methods, and apparent (but yet to be proved) ease of application. The approach can yield a statistical evaluation over any or all parts of the scene as contrasted to the localized data obtained from isolated ground targets.

Theory of Method

Power spectrum analysis can be defined as the decomposition of a random signal into its Fourier components and a comparison of the relative strength or *power* of each frequency component. It has been useful in many applications and is particularly suited to optical images where Fourier analysis is well established. The concept of a random image is used here to include the effects of noise and the possibility of defining statistical sets of similar scenes, e.g., agricultural scenes, coastline scenes, etc.

To develop the necessary theory for the method, consider an optical system forming an image of the ground scene (Figure 1). We can use a generalized Fourier transform relationship to define the power spectrum of each:[3]

$$G_i(f) = \lim_{L_i \to \infty} (1/L_i) \left| \int_{-L_i/2}^{L_i/2} i(x) e^{-i2\pi xf} \, dx \right|^2 = |I(f)|^2$$

$$G_o(f) = \lim_{L_o \to \infty} (1/L_o) \left| \int_{-L_o/2}^{L_o/2} o(x) e^{-i2\pi xf} \, dx \right|^2 = |O(f)|^2$$

where x and f in the object have been scaled by the ratio and inverse ratio, respectively, of Gaussian focal length to flight altitude, to correspond with x and f in the image. L_i and L_o are the spatial extent of the image and object, respectively, f is the spatial frequency variable, and

$$i(x) \Leftrightarrow I(f)$$
$$o(x) \Leftrightarrow O(f)$$

are Fourier transform pairs.

We note two facts about the power spectrum: (1) all spatial phase information in the signals is lost in the squaring operation; i.e., $G(f)$ is real; (2) the power spectrum can be shown to be the Fourier transform of the symmetric autocorrelation function

$$G(f) \Leftrightarrow C(\Delta x)$$

where

$$C(\Delta x) = \lim_{L \to \infty} (1/L) \int_{-L/2}^{L/2} q(x) q(x + \Delta x) \, dx$$

and $q(x)$ is the signal.

Now if we assume the lens to be a linear shift-invariant system[4], the spatial frequency contents of the object and image are related by the *transfer function* of the lens

$$I(f) = T(f)O(f).$$

Taking the complex square, we have

$$I(f)I^*(f) = T(f)T^*(f)O(f)O^*(f)$$
$$|I(f)|^2 = |T(f)|^2 \, |O(f)|^2$$
$$G_i(f) = |T(f)|^2 \, G_o(f).$$

Thus, *the reduction in strength, from object to image, of a frequency component* f *is a measure of the modulus squared of the complex transfer function.*

A more detailed theoretical discussion and an example of the application of the technique for the evaluation of the Apollo 9 multiband cameras has been presented elsewhere.[5]

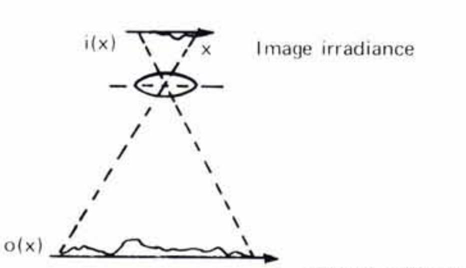

FIG. 1. Diagram of the photography of a ground scene.

Experimental Approach

To measure the transfer function of an operational imaging system in orbit we need to know the spectrum of the ground scene. This can be obtained from simultaneous photography from high-altitude (HA) underflights of the spacecraft. We can make microdensitometric scans of the same ground area on both sets of photographs, as shown in Figure 2. The relative lengths of the scans are determined by the scale between the images so that the same ground area is scanned in both the high-altitude and the

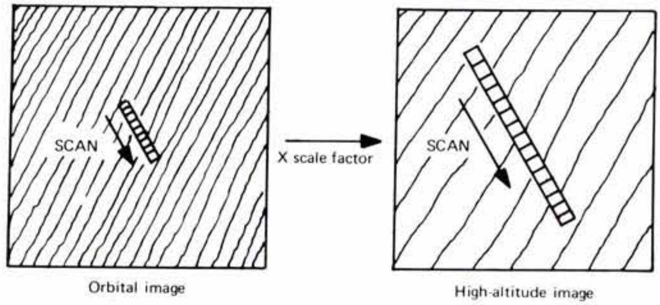

FIG. 2. The scale relationship used in microdensitometric scans of orbital and high-altitude photographs of the same scene taken simultaneously.

orbital photography. A slit should be used for scanning to provide: (a) adequate S/N from the microdensitometer electronics; (b) an average in each measurement of many film grains and several spread functions of the image-forming optics along the length of the slit. This should provide statistically sound values at each point.

Now the spatial frequencies of the scene are scaled from one set of imagery to the other. For example, the Earth Resources Experiment Package (EREP) S190 and S192 experiments on *Skylab* will orbit at an altitude of 435 km. If we underfly these systems with similar optics (i.e., same focal length) at 15 km, the scale factor will be about 29. If we are interested in frequencies up to 120 cycles/mm in the *Skylab* imagery, we need to know the modulation in the HA imagery only up to 4 cycles/mm. The experiment is thus relatively insensitive to the quality of the HA optical system.

Because of this insensitivity we will assume that the performance of the HA system can be described by the laboratory MTF. This could be measured by using a suitable transparency (e.g., with frequencies up to 4 cycles/mm after imaging by the system) as a test object. The same areas of the transparency and its image would be scanned as above, and the ratio of the spectra would be the transfer factor. It is important to note that this transfer factor is an average of the transfer function over the entire scan distance.

The power spectrum of the HA image is now divided by this transfer function (modulus squared) to obtain

$$G_{i_f}(\text{HA})/|T_{\text{lab}}|^2 = G(\text{ground scene}) \times |T_{\text{atmosphere}}|^2.$$

The spectrum of the orbital image is

$$G_{i_f}(\text{orbit}) = G(\text{ground scene}) \times |T_{\text{atmosphere}}|^2 \times |T_{\text{orbit}}|^2.$$

The ratio gives

$$|T_{\text{orbit}}|^2 = G_{i_f}(\text{orbit}) \times |T_{\text{lab}}|^2/G_{i_f}(\text{HA}).$$

We have assumed that, because both systems are outside the atmosphere, $T_{atmosphere}$ is identical for each.

Inasmuch as the Earth Resources Technology Satellite (ERTS) return-beam vidicon (RBV) and multispectral scanner (MSS) and the EREP S190 and S192 experiments will each have as its final product a photographic image, the above techniques are applicable to each system. The essential requirements are: (1) knowledge of the lab T for the HA system (as measured above) and its spectroradiometric characteristic across the region of the scans, and (2) precise sensitometry of the recording film, to permit calibration of exposures.

CONCLUSIONS

The sensor MTF data obtained in this measurement program can be related to the sensor's usefulness to the earth scientist in several ways. We will describe only two here; other generally more complicated schemes will occur to the reader if, for example, he considers different spectral distributions for target and background in conjunction with a multiband MTF for the sensor. In this regard, we can note that the definition of multiband MTF should be analogous to that of multiband resolution.[6]

Let us consider first the results that might be obtained for the various spectral bands of a particular sensor. If the sensor is a film camera, we can expect the infrared MTF to be lower than that in the visible because of the relatively poor MTF for infrared film. As we will see below, we might purposefully decide to design the sensor to have a better MTF in the green than in the red. We can then plot some measure of the information-recording capacity of the sensor, such as the

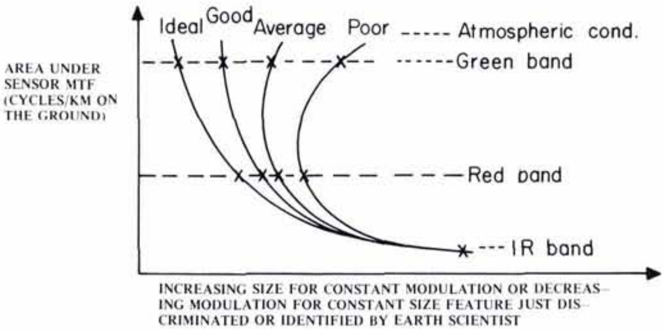

FIG. 3. Sensor performance as a function of spectral band and atmospheric conditions.

area under the sensor MTF curve,[7] against increasing size or decreasing modulation of the feature of interest, as in Figure 3. The left-hand curve corresponds to the results that might be obtained in the absence of a scattering atmosphere. As the atmospheric conditions worsen, the shorter wavelength bands are affected first and the effectiveness of the high MTF of the sensor in the green band is more than offset by the modulation reduction of the atmosphere.

Now let us consider Figure 4 where, for the same ordinate and abscissa as in Figure 3, we can compare the effectiveness of four sensors *A*, *B*, *C* and *D* such as the ERTS RBV and MSS and the EREP S190 and S192 experiments on *Skylab*. The comparison can again be made as a function of atmospheric condition and spectral band.

We should note that the hypothesized results of Figures 3 and 4 would apply to one particular machine-aided photointerpretation technique although the shape, if not the position, of the curves should be independent of the particular technique used. The atmospheric conditions could be broadly classified by ground-based observers as the imagery is being collected. Thus, the conditions could be described as *good*, *average*, etc. for a given area at a given time of day and year. If these classifications prove inadequate, we could extract specific input data from an experiment designed to correct spectral signatures for atmospheric effects.

As the MTF of an image-recording system can be predicted at the design stage, we can now predict how modifications to the design will influence the value of the system to the earth scientist. The results will be immediately applicable to specifying future requirements for sensor design and performance.

We believe that this approach to the analysis of earth resources imagery will provide some of the important basic data needed by those responsible for the planning of earth resources missions. We should emphasize that it can be realized only with the cooperation of:

- The mission planners, in planning simultaneous aircraft underflights with ERTS and *Skylab*, using well-calibrated cameras with wavelength passbands identical to those of the spacecraft sensors.

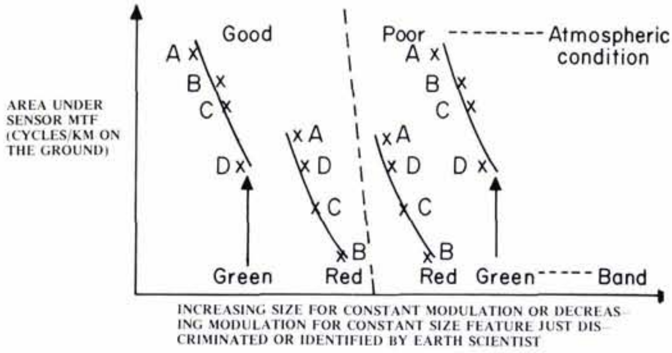

FIG. 4. Comparison of performances of various sensors as a function of spectral band and atmospheric conditions.

- The film processing laboratory staffs, in providing precision processing, sensitometry, and microdensitometry.
- Earth scientists, to provide as accurate a determination as possible of the utility of the spacecraft imagery.

References

1. P. Rosenberg, "Resolution, detectability and recognizability," *Photogram. Eng.* 37(12): 1255–1258, 1971.
2. Committee on Space Programs for Earth Observations, National Academy of Sciences—National Research Council, Division of Earth Sciences.
3. H. J. Zweig, "Autocorrelation and granularity. Part I. Theory," *J. Opt. Soc. Am.* 46(10): 805–811, 1956.
4. J. W. Goodman, *Introduction to Fourier Optics*, McGraw-Hill, New York, 1968, pp. 18–21.
5. R. A. Schowengerdt and P. N. Slater, "Determination of the inflight OTF of orbital earth resources sensors," IX Congress for the International Commission for Optics, Santa Monica, Calif., Oct. 1972.
6. P. N. Slater, "Multiband Cameras," *Photogram. Eng.* 38(6):543–555, 1972.
7. E. L. O'Neill, *Introduction to Statistical Optics*, Reading, Mass., Addison-Wesley, 1963, p. 107.